

# CRICKET INSPIRED HAIRS ON SUSPENDED MEMBRANES WITH CAPACITIVE DISPLACEMENT DETECTION

J.J. VAN BAAR, M. DIJKSTRA, R.J. WIEGERINK, T.S.J. LAMMERINK  
AND G.J.M. KRIJNEN

MESA<sup>+</sup> Research Institute, University of Twente  
P.O. Box 217, 7500 AE Enschede, The Netherlands  
J.vanBaar@el.utwente.nl

**Abstract** — This paper presents the fabrication of artificial hairs of silicon nitride and SU-8 on suspended membranes for flow sensing applications. The suspended membranes contain electrodes for capacitive sensing of the rotation of the hairs. For the silicon nitride hairs a silicon wafer is used as mould and for SU-8 hairs a thick layer was spun. Capacity-voltage measurements have been carried out.

**Key Words:** artificial hair, SiRN, SU-8, capacitive read out

## I INTRODUCTION

Flow velocity can be measured in various ways, e.g. thermally by using a hot wire [1], by measuring the pressure drop in a channel [2] and by measuring the drag force on an obstacle [3]. The latter is used for the artificial hair sensors presented in this paper, which are based on the flow-sensing hairs on the cerci of a cricket. Crickets have hairs with various length and diameter for perception of approaching predators [4].

Several groups have been working on the realization of artificial hairs for flow sensing [5-10]. Two basic types of artificial hairs can be distinguished, namely hairs fabricated in the wafer plane and hairs fabricated perpendicular to the wafer plane. Fabrication of hairs in the wafer plane is most straightforward since surface micromachining techniques can be used [6]. However, surface micromachined hairs are less interesting, because they cannot easily be combined into high-density arrays. Li et al proposed to use the so-called plastic deformation magnetic assembly (PDMA) method to erect the hairs out of the wafer plane [7-9]. In the PDMA process, a magnetic field is used to bend surface micromachined beams. The beams are plastically deformed, so that they remain bent after the magnetic field is removed.

Our research has focused on fabrication of hairs perpendicular to the wafer surface. Two fabrication routes have been investigated. In the first route, a silicon wafer is used as mould to realize silicon-nitride (SiRN) hairs as indicated in Figure 1. In this way a high density of hairs can be realized. The diameter of the hair is independent of the thickness of the SiRN layer. The second fabrication route uses hairs of SU-8

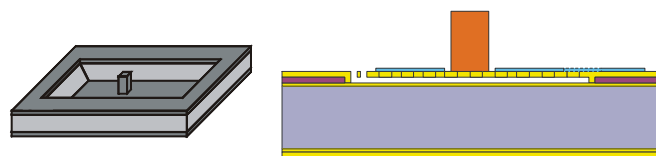
photoresist. These hairs can be realized on top of a surface micromachined read-out structure just before the final release step.



Figure 1. Moulding of a SiRN hair: etching holes in silicon, covering by SiRN and finally removing silicon.

## II DESIGN

Some test runs have been performed where hairs are realized on a membrane as indicated in Figure 2(a). A silicon frame supports the membrane. Hairs with a large diameter have two advantages: it takes less time to etch them by Deep Reactive Ion Etching (DRIE) and the drag force is larger due to the larger frontal area. A disadvantage is the large mask opening. Large holes in the wafer surface prevent proper spinning of resist and complicate further processing steps.



a) silicon frame with SiRN hair on membrane

b) SU-8 hair on suspended membrane with read-out

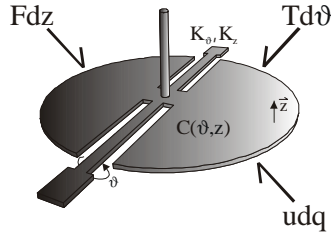
Figure 2. SiRN hair without (a) and SU-8 hair with (b) read out.

Figure 2(b). shows a schematic drawing of a surface micromachined suspended membrane with a hair of SU-8. The device does not have a protective shielding plate above the membrane in order to protect it from the airflow, so that only the drag force on the hair will be measured.

## III MODEL

Figure 3 shows a schematic drawing of a gimbal-suspended sensory hair with capacitive read-

out. The structure can be described by a three-port transducer model: two mechanical ports for rotation and translation of the structure and the third electrical port is the parallel plate condenser. The parallel plate capacitors are formed by the electrodes on the movable plate and by a counter electrode below the moveable plate.



**Figure 3. Three-port transducer model describing artificial sensory hairs.**

The energy of the transducer is given by:

$$E(\vartheta, z, q) = \frac{1}{2}K_{\vartheta}\vartheta^2 + \frac{1}{2}K_z z^2 + \frac{q^2}{2C(\vartheta, z)} + E_b \quad (1)$$

$K_{\vartheta}$  accounts for the torsional spring stiffness of the suspension springs and  $K_z$  accounts for the translational spring stiffness. It is assumed that translation and rotation are linear and independent of each other.

Force balance and torque balance equations are obtained by differentiation of equation (1) with respect to  $\vartheta$  and  $z$ :

$$\begin{aligned} T_{ext} &= \left( \frac{\partial E(\vartheta, z, q)}{\partial \vartheta} \right)_{z, q} = K_{\vartheta}\vartheta - \frac{1}{2}u^2 \frac{\partial C(\vartheta, z)}{\partial \vartheta} = T_{drag} \\ F_{ext} &= \left( \frac{\partial E(\vartheta, z, q)}{\partial z} \right)_{\vartheta, q} = K_z z - \frac{1}{2}u^2 \frac{\partial C(\vartheta, z)}{\partial z} = 0 \end{aligned} \quad (2)$$

$T_{drag}$  enters the equation as the driving force for rotation. Since no analytical expressions were available for  $C(\vartheta, z)$ , the equations (2) were solved simultaneously using MATHLAB.  $K_z$  was calculated from the deflection curve of a beam clamped on both sides, with a point load at the centre of the beam.  $K_{\vartheta}$  was calculated by using Saint-Venant's approximation for a beam under torsion.

Figure 4 shows the calculated capacitance as a function of constant drag-force on the hair for a gimbal-suspended sensor with a plate diameter of  $200 \mu\text{m}$  and a gap distance of  $2 \mu\text{m}$  for various applied voltages. Figure 5 shows calculated C-V curves for the same device, but without applying drag force.

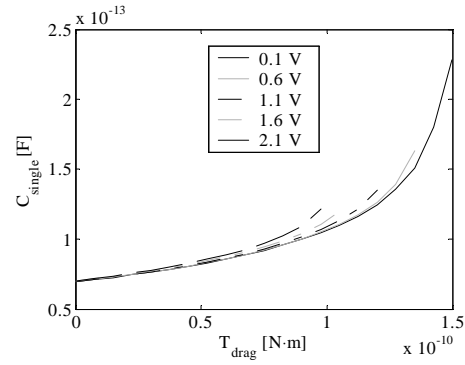


**Figure 4. Capacitance values as a function of constant drag-force on the hair, calculated for a number of voltages.**

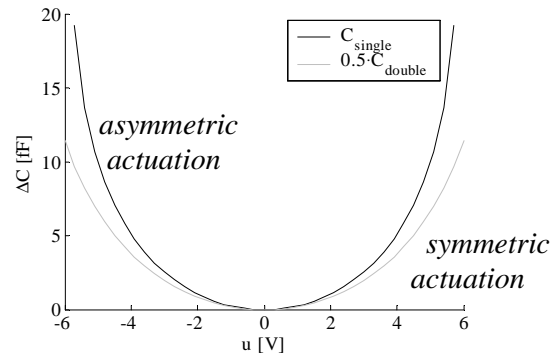


**Figure 5. Calculated capacitance change as a function of applied bias voltage.**

## IV FABRICATION

### A) Silicon Nitride hairs using Si-Moulds

Figure 6 shows the summary of the fabrication process that was developed for the fabrication of artificial hairs by filling holes created by deep reactive ion etching (DRIE).

First, a  $20 \text{ nm}$  thin SiRN layer has been deposited by low-pressure chemical vapor deposition (LPCVD) on a  $0.5 \text{ mm}$  bare  $\langle 100 \rangle$  silicon wafer as an adhesion layer for the  $20 \text{ nm}$  sputtered chromium layer. Between lithography and etching of the chromium layer an ozone step was required for a better wetting of the small pores; otherwise the chromium was not etched. Next, the deep holes are realized by DRIE. These holes are then filled by a  $1 \mu\text{m}$  thick low-stress LPCVD silicon-nitride layer. Finally, the silicon bulk is etched away from the backside using KOH so that the hairs on a membrane are exposed.

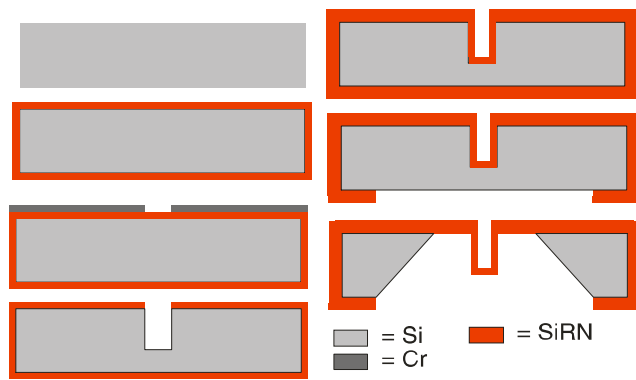


**Figure 6. Process sequence of hair on membrane.**

From the SEM photographs in Figure 7 can be seen that the cross pattern develops into a circular shape and the star shape into a square. Finally all mask openings will end up into a square due to the anisotropy of the <100> Si wafer.

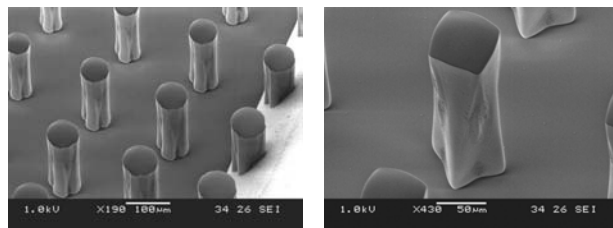


**Figure 7. SEM photographs of hairs with a cross or star shaped opening, developing into a rectangular shape.**

Due to the RIE lag the hair heights ranged from 100 up to 250 micron after 3 hours of DRIE, see Figure 8. The flat top and negative tapering indicate that continued etching will result in longer hairs.

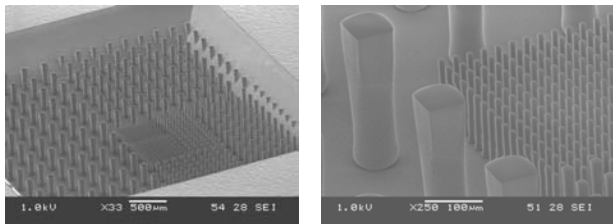


**Figure 8. Hairs with varying diameters of the mask openings (5-50 micron) and therefore varying height.**

## B) SU-8 hairs with read-out

Processing of the complete sensor structures with capacitive read out starts with a highly conductive silicon wafer that will be used as one of the electrodes of the capacitor (9a). A thin silicon nitride layer of 100 nm is deposited as a protection layer for the underlying

silicon (9b). A 1 µm thick LPCVD poly-silicon layer that defines the gap between the membrane and the substrate is deposited (9c) and patterned (9d). Next, a 1 µm LPCVD silicon nitride layer is deposited and patterned which forms the suspension springs and the moveable capacitor (9e,f). Chromium electrodes of 20 nm are sputtered and patterned on top of the silicon nitride (9g).

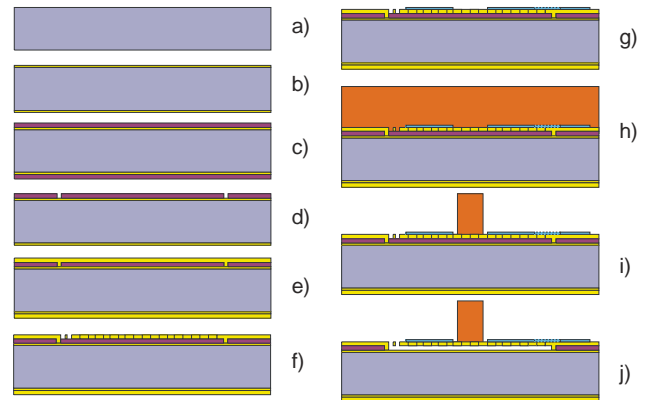


**Figure 6. Process scheme of an SU-8 hair on top of a suspended SiRN membrane with chromium electrodes.**

A thick SU-8 layer is spin-coated on the surface (9h). For the first devices a layer thickness of 200 µm was chosen. It is expected that further optimization is possible to result in a layer thickness (and hair length) of 500 µm [11]. Next, in step i, the SU-8 is illuminated with the hairs pattern and developed. The result are hairs of 50 µm diameter and 200 µm long. Finally the devices are released by plasma etching of the poly-silicon sacrificial layer (9j). Figure 10 shows a SEM photograph of a membrane with four top electrodes.

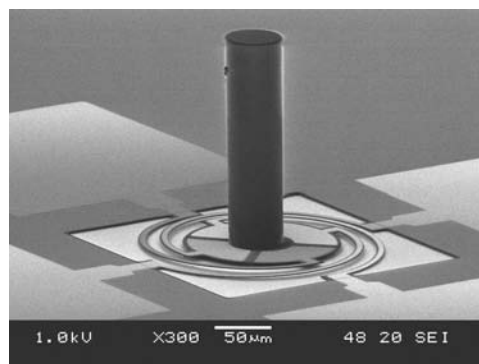


**Figure 10. SEM photograph of SU-8 hair on top of a suspended SiRN membrane with Cr electrodes.**

## V MEASUREMENTS

C-V measurements were done for electrical characterization of the devices, using a HP 4194A impedance analyzer. Two types of measurements were performed. At first the bias voltage was applied to all the electrodes on the device. This gives a symmetric electrostatic force towards the silicon bulk and therefore a translation directed downwards. Secondly, the bias voltage was applied to only half of the electrodes on the device. This results in both rotation and translation of the device.

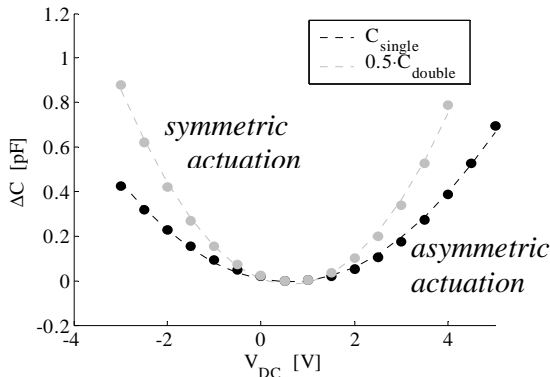


**Figure 11.** C-V measurements on an array of spiral-suspended sensory hairs.

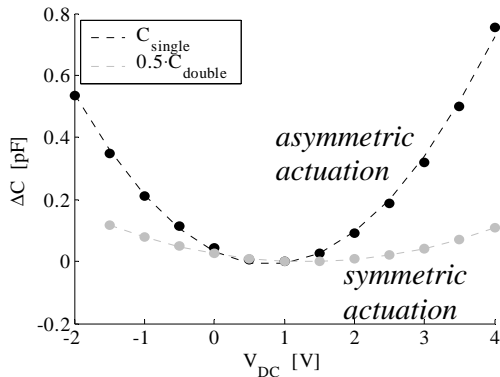


**Figure 12.** C-V measurements on an array of gimbal-suspended sensory hairs.

Figures 11 and 12 show C-V measurements where the effect of translational and rotational movements can be observed in the change in capacitance. It can be seen that the capacitance change for spiral-suspended sensors is slightly smaller when only half of the device is actuated. This means that the device translates more easily than it rotates. Gimbal-suspended sensors show an opposite behavior: the changes in capacitance are smaller when the device is actuated completely.

## VI CONCLUSIONS

We have shown two process schemes for fabrication of arrays of hairs for drag force sensing. The fabrication of a hairs on a membrane by filling deep etched holes turns out to be much more complicated than putting SU-8 hairs on top of a membrane. The SU-8 hairs are now 200 micron high, but will be higher in the future.

## ACKNOWLEDGEMENTS

The authors want to thank: Erwin Berenschot and Meint de Boer for their advice on processing, Rik de Boer for realization of the devices, our colleagues in the EU project CICADA for stimulating discussions and input to this work and the EU for financing support through project IST-2001-34718 (CICADA) in the Lifelike Perception program.

## REFERENCES

- [1] G.C.M. Meyer and A.W. van Herwaarden, *Thermal sensors*, Institute of Physics Publishing, ISBN 0-7503-0220-8.
- [2] F.P. Incropera and D.P. DeWitt, *Fundamentals of Heat and Mass Transfer*, John Wiley 1996.
- [3] F.M. White, *Fluid Mechanics*, McGraw-Hill, 1994
- [4] O. Dangles, J. Casas, Institut de Recherche en Biologie de l' Insecte, private communication.
- [5] Y. Ozaki, T. Ohyama, T. Yasuda, and I. Shimoyama, "An air flow sensor modeled on wind receptor hairs of insects," *Proc. MEMS 2000* (Miyazaki, Japan), pp. 531–537, 2000.
- [6] J. Li, J. Chen, C. Liu, "Micromachined biomimetic sensor using modular artificial hair cells," *Nano Space 2000* (Houston, USA), 2000.
- [7] J. Zou, J. Chen, C. Liu, "Plastic deformation magnetic assembly (PDMA) of out-of-plane microstructures: technology and application," *IEEE/ASME Journal of MEMS*, Vol. 10, Nr. 2, pp. 302–309, 2001.
- [8] Z. Fan, J. Chen, J. Zou, D. Bullen, C. Liu, and F. Delcomyn, "Design and fabrication of artificial lateral line flow sensors," *Journal of Micromechanics and Microengineering*, 12, pp. 655–661, 2002.
- [9] J. Chen, Z. Fan, J. Zou, J. Engel, and C. Liu, "Two dimensional micromachined flow sensor array for fluid mechanics studies," *Journal of Aerospace Engineering*, Vol. 16, No. 2, pp. 85–97, 2003.
- [10] O. Rudko, *Design of a low-frequency sound sensor inspired by insect sensory hairs*, M.Sc. thesis, State University of New York at Binghamton, Department of Mechanical Engineering, 2001.
- [11] [http://www.microresist.de/su-8\\_en.htm](http://www.microresist.de/su-8_en.htm)